Towards Analysis of the Bowing Effect on Burnt Nuclear Fuel Compositions Using SERPENT

Jiazhi Li, Dimitri Rochman, Jose Herrero, Hakim Ferrouki, Alexander Vasiliev, Andreas Pautz

Reactor Physics and Systems Behaviour Laboratory, Paul Scherrer Institute, Villigen, Switzerland
jiazhi.li@psi.ch, dimitri-alexandre.rochman@psi.ch, jose-javier.herrero@psi.ch, hakim.ferroukhi@psi.ch, alexander.vasiliev@psi.ch, andreas.pautz@psi.ch

INTRODUCTION

Nuclear fuel research has some specificities mainly due to the high irradiation environment in the reactor core. Fuel materials under high irradiation undergo unique behaviors such as growth and creep, which can result in bowing of fuel rods [1]. The fuel rod bow can lead to the contact of neighboring rods and shrink water regions between them.

As a consequence, local changes on water moderation in Light Water Reactors (LWR) might affect the isotopic concentrations and their distributions with burn-up. However, in most computational models, the bowing effect on fuel rods is not taken into account [2]. It is therefore essential to investigate the influence of bowing on nuclear computations in general and on assembly depletion in particular. The latter is the topic of primary interest in this paper.

This paper investigates the relative difference of isotopic concentrations induced by bowing to provide a qualitative overview of the effect of bowing via moderation on depletion and build-up of isotopes through burn-up in the fuel rod. Moreover, it illustrates relative isotopic concentrations differences in the perspective of evaluating biases between computational simulation results and the experimentally measured results.

METHODOLOGY

The SERPENT Monte Carlo burn-up code is employed to study the impact on the isotopic evolution of the deformed fuel rods. SERPENT implements the continuous energy Monte Carlo method for solving neutron transport problem, coupled with the CRAM method to solve the Bateman equations [3]. As long as a guess fission source distribution and an estimated initial K-eff value are given, Monte Carlo methods implement single-generation random walk methodology to calculate new neutron distributions and K-eff. During the iterative calculations, the convergence of both the source distribution and K-eff are achieved [4].

A deformed and not deformed fuel structure of 3x3 pin-cells lattice are modeled with SERPENT. Two simulations are launched with the only difference of switching the central normal fuel rod in the lattice into a deformed one. Fuel rod deformation is kept constant for all burn-up steps, with the same operational conditions, dimensions and initial isotopic concentrations in both cases. The relative difference is defined as the ratio of the changes of isotopic number densities relative to the non-deformed case.

To model the deformation, one can discretize the rod into axial layers and shift each layer's axis according to a typical cubic polynomial function. In order to properly account for the asymmetric moderation effect, it is necessary to subdivide each axial layer into several concentric rings, which are also cut into azimuthal sectors. In Fig. 1, the model configuration and geometry dimensions with a S-shape central rod are represented for the horizontal and vertical geometry profiles.

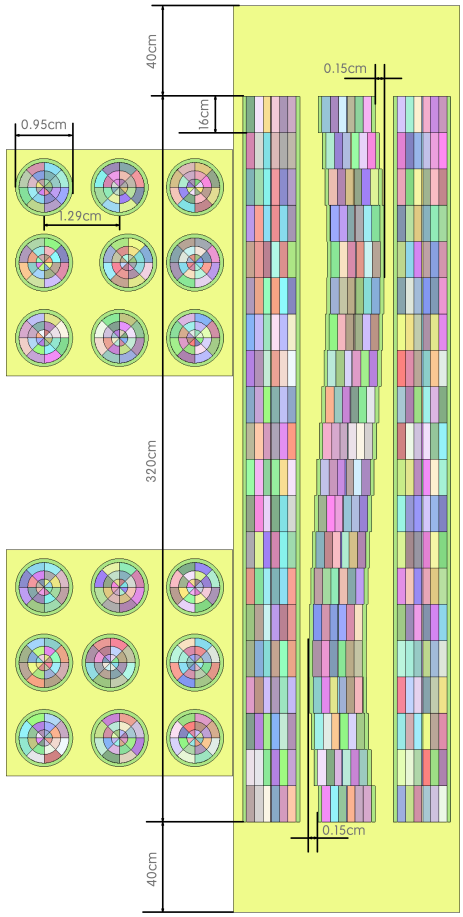

Fig. 1. Horizontal and vertical profiles with a central S-shape deformed fuel rod.

As to the operational conditions, all fuel rods are fresh with 5 w/o enrichment of U-235 assuming for simplicity at the beginning. The cross section, decay and fission yield libraries from ENDF/B-VII.1 are used and the temperature variation in materials is not considered but assumed to be constant, 900 K in fuel and 600 K in moderator. Both simulations are set with periodic boundary conditions in the radial directions and a void boundary at the top and the bottom. 10,000 neutrons, 250 active cycles, 25 inactive cycles and a constant power density of 0.025 kW/g are set up for the SERPENT Monte Carlo simulations.

RESULTS AND ANALYSIS

Though the maximum displacement of 0.15 cm is small compared to the total length of 320 cm, this deformation can lead to notable difference of isotopic number densities for specific axial layers. Three main isotopes, U-235, Pu-239 and Cm-244, are investigated in detail with the purpose of analyzing the bowing effect on isotopic concentrations and their distributions under irradiation. Two simulations are performed with and without deformation. The case without deformation is considered as the reference.

The statistical uncertainties of K-eff are around 30 pcm and the relative statistical errors of power density are up to 1.5%. In Fig. 2, the evolution of relative differences of three isotopes averaged concentrations over the full rods in the 4th and 5th rods between the two cases are plotted against burn-up.

For U-235, one can notice that the relative differences increase almost linearly with burn-up in the 5th rod. Around 0.14% relative difference is observed at the end of burn-up period in the central rod, while the differences are lower in its neighbouring rod.

The negative relative differences in both rods observed in Fig. 2 referring to Pu-239 indicate less production in the case of the deformed rod. Compared to U-235, the relative difference of Pu-239 does not accumulate and reaches around -0.12% at the end of burn-up.

For Cm-244, Fig. 2 shows an ascending evolution of the relative differences from 10 MWd/kgU to 40 MWd/kgU in the 5th rod. It illustrates that less Cm-244 built up at low burn-up after the introduction of a deformed fuel rod in the lattice, while at the end of burn-up around 0.26% relative difference indicates more Cm-244 built up in the full rod.

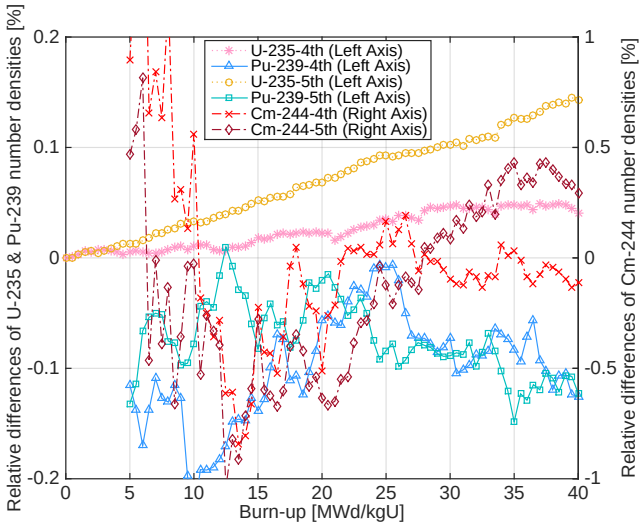

Fig. 2. Relative differences of averaged number densities in the fuel rod between deformed and nominal geometries.

Bowing Effects on Axial Isotopic Concentrations

Instead of averaging isotopic number densities in the fuel rod, further investigations are made on the averaged number densities for every axial layer in the central fuel rod. The relative differences for the axially averaged number densities at 20 MWd/kgU are presented in Fig. 3 for U-235 and Fig. 4 for Pu-239. From the two graphs, one can notice an approximate cosine shape of the averaged number densities. It is due to the higher neutron flux in the central part and is consistent with the realistic conditions in reactor core.

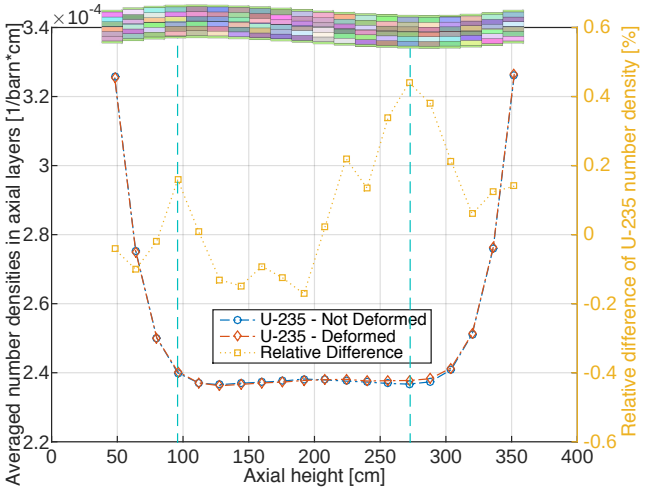

Fig. 3. Axially averaged number densities of U-235 in the central rod at 20 MWd/kgU.

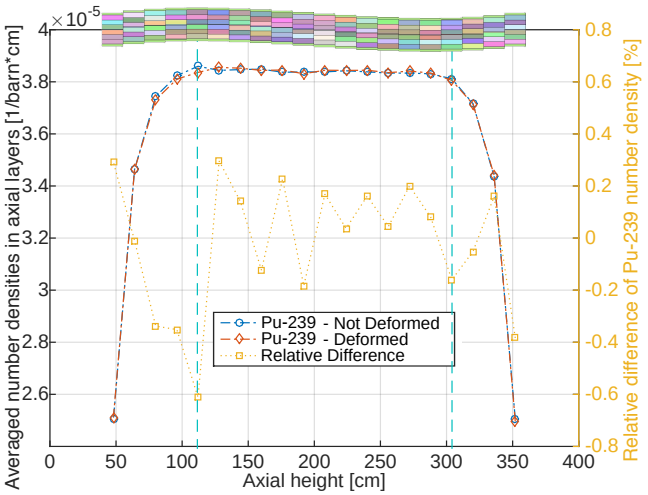

Fig. 4. Axially averaged number densities of Pu-239 in the central rod at 20 MWd/kgU.

The maximum displaced positions are located at the 5th and 16th layers, whose axial positions are 112 cm and 290 cm respectively. It is observable that two peaks (up to 0.4% of the relative difference of U-235) are present in the positive range locating in the 4th and the 15th layer, while two negative peaks appear in the 5th and 17th layers (down to -0.6% for Pu-239). Finally, for Cm-244, two downward peaks also exist and the related results are presented in the following sections.

Intuitively, due to the maximum displacement around the 5th and 16th layers, the distances between fuel rods at

these heights decrease on one side. While on the other side, the deformation enhances the moderation. The moderation variation on two sides normally may cancel out the impact. However, the reduction of moderation on the deformed side dominates the total effect of bowing. Thereby, more U-235 remains in the case with the deformation and less Pu-239 and Cm-244 are built up compared to the case without the deformed rod.

Bowing Effects with Depletion

To study the bowing effect with depletion, the relative differences for the axially averaged number densities in the central rod with the constant bowing along burn-up are plotted.

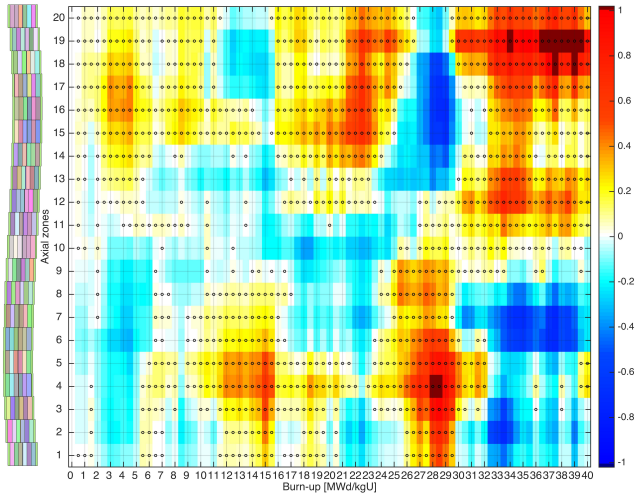

Fig. 5. Relative differences of axially averaged number densities of U-235 along burn-up (Color scale in %).

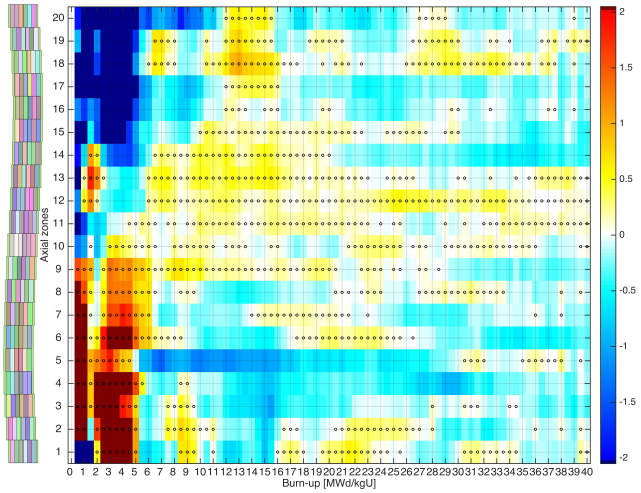

Fig. 6. Relative differences of axially averaged number densities of Pu-239 along burn-up (Color scale in %).

The color scale represents the magnitude of the relative differences in percent and the dots refer to the positive values. In Fig 5, continuous positive relative differences at 4th, 5th, 15th and 16th axial layers from 5 MWd/kgU to 25 MWd/kgU are observed. The magnitude of relative differences seems to accumulate up to 1% with depletion. In Fig 6 and Fig 7, at the 4th, 5th, 16th, 17th layers, it is also observable that negative relative differences are present while the central part from 6th to 15th layers are generally positive. Unlike U-235, Pu-239 and Cm-244 as build-up isotopes keep higher relative differences at the beginning of life and decrease at higher burn-up down to -2% and -8%, respectively.

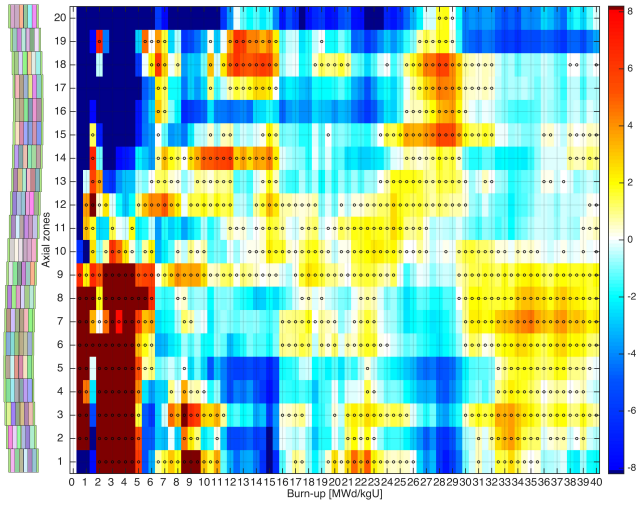

Fig. 7. Relative differences of axially averaged number densities of Cm-244 along burn-up (Color scale in %).

However, in Fig 5 and Fig 7, one can notice the asymmetry of relative differences and the variation is stronger at both low and high burn-up. One simple reason is that there are very low concentrations of Pu-239 and Cm-244 at low burn-up and also relatively low concentration of U-235 at high burn-up. Additionally, it could also originate from a still high statistical uncertainty from the Monte Carlo calculation.

As mentioned before, the relative statistical errors of power density in the simulation are considerable. The flux perturbation contributes to an axially asymmetric power distribution gradually with depletion. Therefore, it continues to lead to an asymmetric shape of isotopic concentrations and their relative differences between two cases. Small burn-up steps and larger amount of neutron histories are essential to obtain the expected axial symmetry during the calculation. In addition, due to the large aspect ratio of the model geometry, it is of great difficulties to obtain a converged neutron source distribution. It has been confirmed in our latest work that in a relatively short model, for instance with the height of 40 cm, a much better convergence of neutron distribution and symmetric isotopic concentrations can be achieved with 50,000 neutrons, 500 active and inactive cycles via a supercomputer. Due to limited computing resources, the work with a 10 times larger model in this paper did not obtain a very good convergence of neutron sources.

Despite of the difficulties to determine the uncertainty of relative differences, it could still be estimated by the axially asymmetric difference of isotopic concentration in the two

cases respectively and the statistical errors of power density distributions.

Bowing Effects on Azimuthal Isotopic Concentrations

A further investigation is performed on the impact of bowing on the azimuthal isotopic number density distributions. With interpolation methods, the isotopic distributions on the section of the 16th axial layer with the maximum displacement at four different burn-up steps are plotted for U-235 in Fig 8. The burn-up steps take 10 MWd/kgU as increment. All graphs are plotted with the same scale and the region surrounded by short vertical lines refers to the boundary of positive relative difference regions.

The narrow water region is located on the right side of the circular section, while on the left the water region is enlarged. In Fig 8, the circular section is generally separated into two parts with positive and negative relative differences. In consequence of two competitive processes of less moderation on the right side and more moderation on the left side, on average due to the hardening neutron spectrum more U-235 remains and less Pu-239 is produced. In addition, the bowing effect has a stronger impact at the pellet periphery compared to the central part. The relative difference accumulates with burn-up and reaches 1.7% locally. Likewise, for Pu-239 and Cm-244, the same investigations are employed and the results are presented in the conclusions.

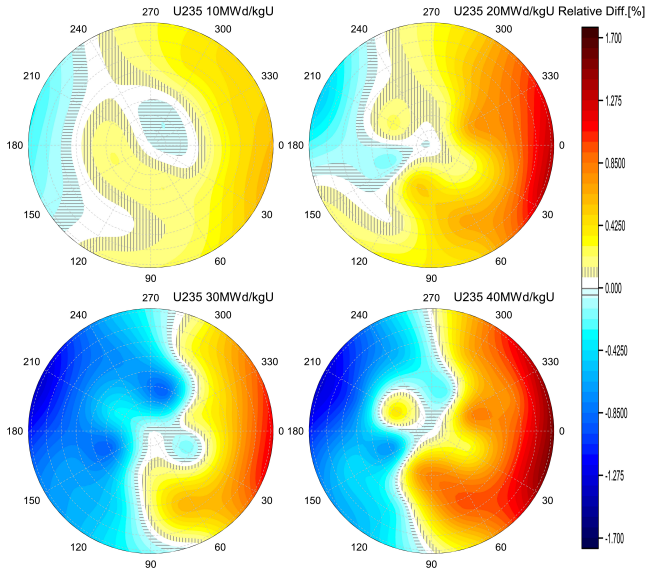

Fig. 8. Azimuthal distributions of the U-235 atomic density relative differences on the section of the maximum displaced layer.

CONCLUSIONS

In this paper, a methodology to investigate bowing effects has been presented. A preliminary test has been performed to illustrate how the methodology could be used to quantify numerical bias for possible safety analyses. The main findings on the relative differences of isotopic concentrations in percent between the two simulation cases (with and without deformation of the central rod in a 3x3 pin-cells lattice) performed in this work are listed in Table I.

Table I. Relative differences of isotopic concentrations.

Relative Difference	[%]	U-235	Pu-239	Cm-244
Avg. in a rod	4th	0.04	-0.12	-0.11
40 MWd/kgU	5th	0.14	-0.12	0.29
Avg. in a layer	Top	0.44	-0.16	-1.39
20 MWd/kgU	Bot	0.16	-0.61	-3.75
With Burn-up	Range	< 1	> -2	> -8
16th Section	Range	< 1.7	> -5.4	> -11.3

The deformation of the fuel rod is defined at the beginning and keeps constant till the end of burn-up. Thus, the estimated relative differences of isotopic concentrations induced by bowing are higher, compared to reality where the deformations evolve during burn-up. However, the maximum displacement of 0.15 cm is relatively small in the model; one could achieve larger relative differences if the displacement increases. Additionally, in view of the axial asymmetry observed in the relative differences, it is necessary to increase neutron histories to obtain a converged neutron distribution.

The progressive deformation with burn-up and convergence studies come to be the future work. Moreover, a C-shape bow is likely to be used because of a plane symmetry. It is known that the bowing deformation normally occurs on fuel assemblies with about 1 cm displacement, which would strongly affects water gaps between them[1]. In case of solving convergence, the work would move towards analyzing bowing effects in multi-assembly models with multiple fuel rods.

ACKNOWLEDGMENTS

This work was conducted in the framework of the Joint Master Program of Nuclear Engineering by ETHZ, EPFL and PSI in Switzerland. Thank Matthias Krack for solving the problem of computational capacities.

REFERENCES

1. V. INOZEMTSEV, *Review of Fuel Failures in Water Cooled Reactors*, pp. 112–127, International Atomic Energy Agency (2010).
2. K. OKUMURA, T. MORI, M. NAKAGAWA, and K. KANEKO, "Validation of a continuous-energy Monte Carlo burn-up code MVP-BURN and its application to analysis of post irradiation experiment," *Journal of Nuclear Science and Technology*, **37**, *2*, 128–138 (2000).
3. J. LEPPÄNEN, "Serpent–a continuous-energy Monte Carlo reactor physics burnup calculation code," *VTT Technical Research Centre of Finland* (2015).
4. F. B. BROWN, "A review of Monte Carlo criticality calculations–convergence, bias, statistics," *Proc. M&C*, American Nuclear Society, New York (May 3-7 2009).